HHS Public Access

Author manuscript

Neurobiol Dis. Author manuscript; available in PMC 2024 February 02.

Published in final edited form as:

Neurobiol Dis. 2023 October 15; 187: 106305. doi:10.1016/j.nbd.2023.106305.

Protein kinase D2 confers neuroprotection by promoting AKT and CREB activation in ischemic stroke

Jaclyn A. Connelly[a], **Xuejing Zhang**[a], **Yuzhou Chen**[a], **Yapeng Chao**[a], **Yejie Shi**[b], **Tija C. Jacob**[a], **Q. Jane Wang**[a,*]

[a]Department of Pharmacology and Chemical Biology, University of Pittsburgh, Pittsburgh, USA

[b]Department of Neurology, University of Pittsburgh, Pittsburgh, USA

Abstract

Ischemic stroke, constituting 80–90% of all strokes, is a leading cause of death and long-term disability in adults. There is an urgent need to discover new targets and therapies for this devastating condition. Protein kinase D (PKD), as a key target of diacylglycerol involved in ischemic responses, has not been well studied in ischemic stroke, particularly PKD2. In this study, we found that PKD2 expression and activity were significantly upregulated in the ipsilateral side of the brain after transient focal cerebral ischemia, which coincides with the upregulation of PKD2 in primary neurons in response to *in vitro* ischemia, implying a potential role of PKD2 in neuronal survival in ischemic stroke. Using kinase-dead PKD2 knock-in (PKD2-KI) mice, we examined whether loss of PKD2 activity affected stroke outcomes in mice subjected to 1 h of transient middle cerebral artery occlusion (tMCAO) and 24 h of reperfusion. Our data demonstrated that PKD2-KI mice exhibited larger infarction volumes and worsened neurological scores, indicative of increased brain injury, as compared to the wild-type (WT) mice, confirming a neuroprotective role of PKD2 in ischemia/reperfusion (I/R) injury. Mouse primary neurons obtained from PKD2-KI mice also exhibited increased cell death as compared to the WT neurons when subjected to *in vitro* ischemia. We have further identified AKT and CREB as two main signaling nodes through which PKD2 regulates neuronal survival during I/R injury. In summary, PKD2 confers neuroprotection in ischemic stroke by promoting AKT and CREB activation and targeted activation of PKD2 may benefit neuronal survival in ischemic stroke.

Keywords

Ischemic stroke; Protein kinase D2; Neuroprotection; AKT; CREB

*Corresponding author at: Department of Pharmacology and Chemical Biology, University of Pittsburgh School of Medicine, E1354 BST, Pittsburgh, PA 15261, USA. qjw1@pitt.edu (Q.J. Wang).

Author contributions

Q.J.W. performed study concept and design; J.A.C, X.Z., Yu.C., Ya.S., T.C.J., and Q.J.W. developed methodology; J.A.C, Y.S., T.C.J., and Q.J. W. performed writing, review and revision of the paper; J.A.C, X.Z., Yu. C., Ya.C., and Q.J.W. provided data acquisition, analysis and interpretation, and statistical analysis; Y.S. and T.C.J. provided technical and material support. All authors read and approved the final paper.

Declaration of Competing Interest

The authors declare no conflict of interest.

1. Introduction

Stroke results from a sudden disruption of blood flow to the brain. Approximately 85% of all strokes are due to cerebral ischemia resulting from embolic or thrombotic occlusion of a major cerebral artery. Despite the availability of two treatment options including tissue plasminogen activator (tPA) and surgical endovascular recanalization, only <30% of stroke patients are suitable for these treatments. Ischemic brain damage centers around the loss of neuronal viability and function. In the event of ischemic stroke, the occlusion of a cerebral vessel causes oxygen and glucose deprivation and ATP deficit, resulting quickly (minutes) in neuronal death in the ischemic core, which is considered beyond rescue. However, the peri-infarct regions (PI, ischemic penumbra) are a transition zone where cell death progresses relatively slower (hours), which is the key target site of most stroke therapies in order to prevent cell death and reduce infarct volume (Yang and Liu, 2021; Zhao et al., 2022). There is a delicate balance of pro-death and adaptive pro-survival signaling events in the peri-lesion regions which ultimately determine the extent of brain damage after acute ischemic injury. The discovery of genes involved in the I/R-induced pro-survival mechanisms may lead to new targets and therapies that promote neuronal survival and recovery after ischemic stroke.

The PKD family with three members, PKD1, PKD2 and PKD3, belongs to a subfamily of the Ca^{2+}/calmodulin-dependent protein kinase superfamily (Zhang et al., 2021). It is an important player in the diacylglycerol (DAG) signaling network that has long been implicated in cerebral ischemia (Bright and Mochly-Rosen, 2005). In the event of rising DAG in cell membranes, PKD is recruited by DAG to those membranes where it is activated directly by co-recruited protein kinase C (PKC) *via* phosphorylation on two conserved serine residues (S744/748 for human PKD1) in the activation-loop. Once activated, PKD activity can be maintained by autophosphorylation independent of PKC. There is growing evidence identifying PKD as a key sensor for a variety of cellular stresses (Zhang et al., 2021). The activation of PKD by these stresses triggers compensatory adaptive responses that serve to protect and strengthen normal cell functions such as cell viability or growth *via* different mechanisms. It has been shown that PKD attenuates oxidative stress-induced cell death by activating the NF-κB transcriptional factor and its pro-survival target genes (Storz and Toker, 2003). PKD also modulates cell survival *via* regulation of other important cell survival and proliferation pathways such as ERK1/2 (Chen et al., 2008; Wei et al., 2014), AKT (Chen et al., 2008; Wei et al., 2014), and heat shock protein 90 (HSP90) (Azoitei et al., 2014). In the brain, PKD has been implicated in neuronal polarity (Higuero et al., 2010; Li and Wang, 2014; Tang, 2001; Watkins et al., 2008; Yin et al., 2008) and a few neural developmental disorders including a potential role of PKD2 in autism spectrum disorder (Matsumura et al., 2019; Zhang et al., 2021). A neuroprotective role of PKD1 has been demonstrated previously (Pose-Utrilla et al., 2017; Stetler et al., 2012). PKD1 confers neuroprotection by binding and phosphorylating heat-shock protein 27 (HSP27), an established cytoprotective target for ischemic brain injury (Stetler et al., 2008). PKD1 was also found to be inactivated by excitotoxicity resulting in the shutdown of a pro-survival IKK/NF-κB/SOD2 pathway to potentiate neuronal death, indicating a protective role of

PKD1 in this context (Pose-Utrilla et al., 2017). Despite these important findings on PKD1, nothing is known about the role of PKD2 or PKD3 in ischemic stroke.

In this study, we evaluated the *in vivo* and *in vitro* function of PKD2 in ischemic stroke and neuronal survival using a kinase-dead PKD2 knock-in mouse model and cultured primary neurons. Our data demonstrated that loss of PKD2 activity aggravated post-stroke brain infarction and increased neuronal death after ischemic stroke. Further analysis indicated that PKD2 contributes to neuronal survival by modulating pro-survival AKT and CREB pathways in neurons.

2. Results

2.1. The expression of PKD isoforms in wildtype (WT) and kinase-dead PKD2 knock-in (PKD2-KI) mouse brain

The activation of PKD is dependent on the phosphorylation of two conserved serine residues (S707/S711 for mouse PKD2) in the activation loop of the catalytic domain (Sturany et al., 2002). To investigate the role of PKD2 in ischemic stroke, homozygous kinase-dead PKD2 knock-in mice were generated by displacing wild-type PKD2 alleles with mutant alleles that encode alanine substitutions at the two serine residues (S707A/S711 A), resulting in a phosphorylation-defective kinase-dead mutant $PKD2^{SSAA/SSAA}$ (PKD2-KI or KI). The PKD2-KI mice have been described previously and the homozygous mice are viable, fertile, normal in size, and do not display any gross physical or behavioral abnormalities (Matthews et al., 2010). Mouse genotyping confirmed the presence of mutated alleles (Chen, 2023). To gain insights in PKD function in the brain, we first analyzed the expression pattens of PKD isoforms in WT and KI mouse brain. As shown in Fig. 1A, all three PKD isoforms were detectable in the whole mouse brain. A slightly higher expression of PKD1 was noted in striatum as opposed to the lower expression of PKD2 and PKD3 in this region. This difference was greatest for PKD2 with almost exclusive expression in the cortex and hippocampus while little was detected in the striatum (Fig. 1B). We also observed a slight upregulation of overall basal p-S473-AKT in dissected KI brain tissues, which could be compensatory events for their reduced activities due to loss of PKD2 activity. Immunofluorescent (IF) staining of the mouse cortex showed that PKD2 was primarily expressed in the cytosol and the PKD2-expressing cells were also stained positive for the neuron marker NeuN (Fig. 1C), clearly demonstrating the expression of PKD2 in cortical neurons.

2.2. PKD2 expression and activity were upregulated by I/R injury

To investigate the role of PKD in ischemic stroke, we first examined PKD isoform expression and activity after I/R injury in a mouse model of transient focal cerebral ischemia. WT and KI mice were subjected to 1 h transient middle cerebral artery occlusion (tMCAO) followed by 24 h reperfusion. Notably, PKD2 mRNA was significantly upregulated in the ipsilateral side of the brain tissues, whereas PKD1 and PKD3 mRNAs were either downregulated or unchanged/mildly upregulated on the ipsilateral side as compared to the contralateral side (Fig. 2A). Accordingly, PKD2 protein was detected at higher levels in the PI regions (penumbra) of the ipsilateral hemisphere as compared to

the contralateral side (Fig. 2B), this correlated to increased PKD activity measured by the p-S744/748-PKD antibody that detects all three active PKD isoforms (Fig. 2B–C). In contrast, the levels of PKD1 and PKD3 protein were similar in the two hemispheres (Fig. 2B). Additionally, IF staining of the peri-infarct region of the cortex showed increased p-S876-PKD2, indictive of activated PKD2, while this signal was absence in WT control and KI MCAO cortices, validating the activation of PKD2 after MCAO and loss of PKD2 activity in the KI mice (Fig. 2D).

To further evaluate the role of PKD2 in neurons, primary rat cortical neurons were prepared from the cerebral cortices of embryonic day 18 rat embryos. The expression of PKD transcripts and proteins was evaluated in rat primary neurons under oxygen-glucose deprivation/reoxygenation (OGD/R) condition to mimic I/R injury *in vitro*. All three PKD mRNAs were upregulated and peaked at 24 h reoxygenation after 1 h OGD (H1R24), among which PKD2 upregulation was most prominent (Fig. 3A). At the protein level, PKD2/3 showed persistent upregulation with PKD2 being the greater, while that of PKD1 was downregulated in response to OGD/R (Fig. 3B–C). The upregulation of PKD2 expression and activity correlated with our observation in mouse brain tissues (Fig. 2). Collectively, these data indicate that PKD2 is the most significantly upregulated PKD isoform in neurons at both transcript and protein levels in response to I/R injury *in vivo* and *in vitro*, implying a potential role in neuronal survival and function.

2.3. Loss of PKD2 activity exacerbated ischemic brain injury

To determine if loss of PKD2 activity affected ischemic brain injury, PKD2-KI and WT mice were subjected to 1 h MCAO followed by 24 h reperfusion. At 24 h reperfusion (before the mice were sacrificed for the TTC staining), an evaluation of neurological motor deficits (neuroscores) was performed. The KI mice showed significantly increased % total infarct volume (30% WT *vs.* 43% KI), which was reflected in increased infarction in both cortical and striatal regions of the brain (Fig. 4A–B) and worsened neurological scores for KI (22.76, $n = 28$) as compared to WT mice (17.57, $n = 27$) ($^{*}P < 0.05$), demonstrating deteriorated neurological and motor functioning (Fig. 4C). Additionally, analysis of mouse survival 24 h after successful MCAO surgery, KI exhibited 31.03% mortality as compared to 7.41% mortality for WT mice, indicating that PKD2 activity is required for mouse survival after ischemic stroke. Collectively, these results suggest that the loss of PKD2 activity in PKD2-KI mice results in increased brain infarction, worsened neurological function, and reduced mouse survival after I/R injury, implying PKD2 protects against ischemic brain injury.

2.4. Inactivation of PKD2 potentiated OGD/R-induced neuronal death

The functional significance of PKD2 on neuronal survival was evaluated using murine primary neurons. The viability of WT and KI mouse primary neurons was evaluated at H1R24 by Calcein-AM/PI staining. The KI neurons were 2× less viable than the WT neurons (Fig. 5A–B). To further this analysis, the neuronal viability at H1R24 was determined in rat primary neurons pre-treated with or without a PKD inhibitor CRT0066101 (CRT), followed by OGD/R in the presence of CRT. CRT is a pan-PKD inhibitor with similar potencies for all three PKD isoforms (Harikumar et al., 2010; Wang and Wipf,

2023). Our data showed that inhibition of PKD significantly exacerbated OGD/R-induced neuronal cell death compared with the vehicle-treated controls (Fig. 5C–D). Thus, PKD2 activity promoted neuronal survival after I/R injury.

2.5. Inactivation of PKD2 attenuated the activation of AKT and CREB by I/R

AKT and CREB were consistently and significantly altered in response to genetic inactivation or pharmacological inhibition of PKD2. Notably, in brain tissues dissected from WT and KI mice 24 h after tMCAO, p-S473-AKT was markedly reduced in the ipsilateral hemisphere of KI mice as compared to that of WT mice (Fig. 6A–B). The levels of activated PKD measured by p-S744/748-PKD was reduced nearly two-fold. The remaining p-S744/748-PKD signal in the KI mouse may have resulted from the activated PKD1 and PKD3 but not PKD2 since it has been genetically inactivated. In mouse primary neurons subjected to OGD/R, p-S473-AKT was reduced in both the early (H1R1) and late phase (H1R24) of OGD/R in the KI neurons as compared to the WT neurons (Fig. 6C–D). Similarly, p-S133-CREB and CREB were also downregulated in KI as compared to WT at H1R1 and H1R24 (Fig. 6C–D). These correlated to the increased apoptosis in the KI neurons as indicated by the increased cleaved caspase 3, an apoptosis marker (Fig. 6C).

To further evaluate the causal relationship between PKD, AKT, and CREB, we turned to N2a, a cultured mouse neuronal cell line. N2a only expressed PKD2, but not PKD1 and PKD3, confirmed at both transcript and protein levels (Fig. 7A–B). Similar to primary neurons, N2a cells subjected to OGD/R treatment also exhibited persistent upregulation of PKD2 at mRNA and protein levels, accompanied by increased PKD2 activity measured by the p-S744/748-PKD antibody (Fig. 7B–C). Next, we examined if pharmacological inhibition of PKD by CRT could affect the downstream signaling pathways. CRT was added throughout the course of OGD/R treatment. Notably, CRT most significantly blocked AKT activation at H3R0 and H3R24 (Fig. 7D–E), consistent with the attenuated AKT phosphorylation in the KI neurons at the early and late phase of OGD/R (Fig. 6C–D). Accordingly, overexpression of a Flag-tagged mouse PKD2 in N2a cells resulted in elevated AKT and CREB phosphorylation before and after OGD/R treatment (Fig. 7F–G), indicating a significant role of PKD2 in regulating AKT and CREB activation, particularly at early time points where excitotoxicity takes place. Next, the effects of PKD2 overexpression on the proliferation/viability of N2a cells stably expressing a cell viability red fluorescent marker NucLight Red (NR) marker were examined by real-time live-cell imaging. Note that OGD induces progressive cell death of N2a in early phase (0–24 h), followed by a proliferative phase where N2a cells recover and resumes normal growth. Overexpression of PKD2-Flag promoted the survival and proliferation of N2a after OGD/R ($p < 0.0001$, ANOVA) (Fig. 7H–I). The causal effect of PKD-induced AKT activation on neuronal viability was also examined by treating the cells with a pan-AKT inhibitor AZD5363 (capivasertib). As shown in Fig. 7H, AZD5363 significantly blocked PKD-induced increase in N2a cell survival and proliferation ($p < 0.0001$, ANOVA), indicating a key role of AKT in mediating the pro-survival effects of PKD2 in neuronal cells. Taken together, our data demonstrated a causal role of PKD2 in promoting I/R-induced AKT and CREB activation and neuronal viability during the early phase of ischemic injury.

3. Discussion

Ischemic stroke accounts for the majority of stroke cases in the world. It occurs when a blood vessel that supplies the brain is abruptly blocked, causing severely reduced cerebral blood flow, deprivation of oxygen and nutrients in affected brain tissues, and induction of excitotoxicity. When the blood flow is subsequently restored by clot lysis, it triggers secondary oxidative damage and post-ischemic inflammation, ultimately leading to neuronal cell death and brain infarction. There is still incomplete understanding of the molecular underpinnings of ischemic stroke and the treatment options have not been advanced for decades. In this study, we sought to delineate the function and signaling mechanisms of the PKD kinases in ischemic stroke-induced neuronal damage in the brain, mainly focusing on the PKD2 isoform. Using a PKD2 kinase-dead knock-in mouse model, we demonstrated for the first time a protective role of PKD2 in a mouse model of ischemic stroke. Genetic inactivation of PKD2 exacerbated brain injury resulting in increased infarction volumes and worsened neurological scores in mice subjected to tMCAO. Our data also demonstrated selective upregulation of PKD2 expression and activity in the peri-lesion areas of mouse brain after tMCAO and in cultured primary cortical neurons after OGD/R. Loss of PKD2 activity reduced neuronal survival in primary neurons, indicating a neuron-specific role of this kinase in survival. Further study showed that this effect was mediated through modulating AKT and CREB activities after I/R injury.

Our data showed that all three PKD isoforms were detected in cortex, hippocampus, and striatum. However, there are differences in their expression in different regions of the brain, for example, PKD2 was higher in the cortex and hippocampus but lower in striatum (Fig. 1A). Importantly, upon induction of ischemic stroke, PKD2 transcripts were increased in the ipsilateral side of the brain, correlating to higher levels of PKD2 protein and activity in the PI regions and cortex (Fig. 2A–C), indicating that I/R induced the activation of PKD2 in the peri-infarct region. There were some unexpected changes of PKD1 transcript and protein levels in the mouse tissue and primary neurons, for example we observed the upregulation of the *Prkd1* transcripts but the PKD1 protein levels appeared to be downregulated in the primary neurons (Fig. 3). It is possible that other post-transcriptional mechanisms may affect PKD1 expression after I/R. PKD2 has been detected at high levels in neocortex and other regions of the mouse brain during the later stages of embryogenesis (Atik et al., 2014; Oster et al., 2006). PKD2 has also been detected in cortical and hippocampal neurons in mouse brain, but in these studies PKD1 protein was found to be more abundant than PKD2 as detected by a PKD1/2 antibody (Avriyanti et al., 2015; Pose-Utrilla et al., 2017), while we used a mouse PKD2-specific antibody, which might explain the discrepancies observed in these studies.

Despite the growing knowledge of PKD in various biological systems, most studies focus on the PKD1 isoform, while the roles of PKD2 and 3 remain largely elusive, particularly in the central nervous system. Our study is the first that demonstrated a neuroprotective role of PKD2 in response to I/R injury. Two previous reports have also implicated PKD1 in ischemic stroke (Pose-Utrilla et al., 2017; Sanchez-Ruiloba et al., 2014; Stetler et al., 2012). Thus, based on our findings and those of others on PKD1, it appears that PKD1 and 2 are both neuroprotective in response to I/R injury. This is further supported by our

findings (Fig. 5) and other reports that pan-PKD inhibitors, such as CID755673 (Stetler et al., 2012) and CRT0066101 (Pose-Utrilla et al., 2017), decreased neuronal survival under ischemic or excitotoxic conditions. An important implication of these findings is that pan-PKD activators may have therapeutic values in ischemic stroke. Although many PKD inhibitors have been developed, there have not been any selective PKD activators. Future studies could be directed at developing these novel targeted activators of PKD, either small molecule- or peptide-based therapeutics. The benefits of these PKD-targeted therapeutics are well anticipated.

In this study, we have identified AKT and CREB as two major signaling nodes downstream of PKD2 in I/R injury. This is supported by: 1) p-AKT levels were markedly attenuated in ipsilateral KI brain tissues after tMCAO (Fig. 6A–B); 2) AKT and CREB activation was blocked at 1 and 24 h post-OGD in KI primary neurons, which inversely correlated to increased cleaved caspase 3 (Fig. 6C–D); 3) a PKD inhibitor CRT suppressed OGD/R-induced early activation of AKT in N2a cells (Fig. 7D–E); 4) overexpressed PKD2 enhanced AKT and CREB activation at 1 h post-OGD (Fig. 7F–G). PI3K/AKT and ERK/CREB are key mediators of neuronal survival pathways downstream of *N*-methyl-D-aspartate receptors (NMDARs) in ischemic stroke (Ge et al., 2020; Wu and Tymianski, 2018). PKD1 is known to regulate AKT activity but less is known about PKD2 (Zhang et al., 2021). Inhibition or knockdown of PKD2 has been shown to decrease AKT activity and block tumor cell survival and proliferation in colon cancer cells (Wei et al., 2014) and glioma cells (Zhou et al., 2014). Our findings indicate that PKD2 contributes to AKT activation both in the early (excitotoxicity) and late phase (oxidative stress) of I/R, implying complex regulation, possibly *via* different mechanisms at different stages of I/R injury. CREB is a major transcription factor activated by ischemic injury. Excitotoxicity-induced NMDAR activation and subsequent Ca^{2+} influx triggers CREB activation, leading to expression of genes such as BCL-2 and BCL-x that protect neurons from ischemic insult (Kitagawa, 2007). Our data demonstrated reduction of pro-survival p-S133-CREB in response to OGD/R in KI neurons as compared to the WT neurons and restoration of p-S133-CREB in PKD2-overexpressing N2a cells as compared to the control cells after OGD/R (Fig. 6C–D and 7F–G), indicating a potential role of PKD2 in regulating CREB activity. CREB is also known as a direct PKD substrate (Johannessen et al., 2007). Both PKD1 and PKD2 have been shown to directly regulate CREB transcription by S133 phosphorylation on CREB (Guo et al., 2011). Thus, PKD2 may directly regulate CREB phosphorylation in neurons in response to acute I/R injury.

Our study has two limitations: 1) Only male mice were tested in our study. However, sexual dimorphism is an important factor that affects many aspects of brain's response to stroke or stroke therapies (Chandra et al., 2021; Jia et al., 2022; Liu et al., 2022; Wang et al., 2021). The role of PKD in sexual dimorphism is largely unknown. One report showed that PKD3 played a more significant role in osteoclastogenesis and bone formation in male mice than female mice (Burciaga et al., 2023). Another study on the *Drosophila* PKD homolog found that males were slightly shorter lived and starvation sensitive than females, suggesting males maybe more prone to stress-induced damages (Maier et al., 2019). Additionally, we have previously identified PKD1 as an androgen repressed gene in prostate cancer (Zhang et al., 2017), implying that the level of PKD1 might be lower in males than females, which

may affect their sensitivity to ischemic brain injury. More studies are needed in this area in the future. 2) Another limitation of our study is related to aging as only young mice were examined in our study. Aging is a key modifier of stroke outcome (Gallizioli et al., 2023; Sakamuri et al., 2022; Sommer and Schabitz, 2021; Yousufuddin and Young, 2019). Over 75% of all stroke incidences occur in people aged ≥65 years and are associated with worsened functional outcomes. Aging can influence stroke outcomes by many means including but are not limited to reducing metabolic reserves, diminishing cerebrovascular reactivity, reducing neuronal plasticity, inducing chronic low-grade inflammation, some of which have been linked to aberrant PKD activity or expression (Zhang et al., 2021). Thus, PKD may be targeted to limit age-associated stroke incidence and outcome, which will be investigated in aged animals in our future study.

In summary, our study reveals a novel role of PKD2 in neuroprotection after ischemic stroke. We have not only demonstrated a significant protective role of PKD2 in mouse brain *in vivo*, but also showed that this pro-survival effect resides within the neurons through enhancing AKT and CREB activities. Our study does not exclude the possibility that PKD2 expressed in other brain cell types may also contribute to the neuroprotective mechanisms of PKD2. The identification of PKD2 as a novel regulator of neuronal survival provides new insights into ischemic stroke-associated neuroprotective mechanisms. Our findings may open a new line of inquiry into the development of PKD-targeted therapeutics for neuroprotection after ischemic stroke.

4. Materials and methods

4.1. Reagents and antibodies

The iScript cDNA synthesis kit was obtained from Bio-Rad Laboratories (Richmond, CA, USA). Cell culture reagents and media were from American Type Culture Collection (ATCC, Rockville, MD). The antibodies for PKD1 (90039), PKD2 (8188), PKD3 (5655), AKT (9272), p-S473-AKT (9271), CREB (9197), p-S133-CREB (9198), Cleaved Caspase-3 (9661), and p-S744/748-PKD (2054) were purchased from Cell Signaling Technology (Danvers, MA, USA). The antibodies for mouse PKD2 were obtained from Biomatik (CAU27785, Wilmington, DE, USA) and Santa Cruz Biotechnology (sc-374344, Santa Cruz, CA, USA). The antibodies for Flag (MA1–91878) and p-S876-PKD2 (PA5–40221) was from Thermo Fisher (Waltham, MA, USA). The GAPDH (sc-32233) antibody was from Santa Cruz Biotechnology (Santa Cruz, CA, USA). Goat anti-rabbit and goat anti-mouse HRP-conjugated secondary antibodies were from Bio-Rad Laboratories (1706515 and 1706516, Madison, WI, USA). CRT0066101 (2-[4-[[(2*R*)-2-aminobutyl]amino]-2-pyrimidinyl]-4-(1-methyl-1H-pyrazol-4-yl)phenol dihydrochloride) was obtained from Tocris Bioscience (Bio-Techne, Minneapolis, MN).

4.2. Animals

Catalytic deficient heterozygous PKD2$^{S707A.S711A/WT}$ (PKD2$^{SSAA/WT}$) knock-in mice on a C57BL/6 background were obtained from Jackson Laboratory (Bar Harbor, ME, USA). Homozygous PKD2$^{SSAA/SSAA}$ KI mice were obtained by intercrossing heterozygous PKD2$^{SSAA/WT}$ mice. Mouse genotyping was carried out by PCR amplification of genomic

DNA using the following primers: 5′-AGTGGCACGTTCCCCTTCAATG-3′ (sense), 5′-CTTTGCCCAATCCCTTACAGCCT-3′ (antisense). Wild-type male C57BL/ 6 J mice (8–10 weeks of age) were purchased from Jackson Laboratory. All animal experiments were conducted in accordance with the University of Pittsburgh Institutional Animal Care and Use Committee guidelines. Mice were housed in a temperature-controlled room with 12 h light/dark cycle with standard mouse diet and water *ad libitum* at the University of Pittsburgh animal facility. Male WT and KI (~18–20 g, $n = 5–8$ per group) were used for the MCAO study. To detect a 20% difference with 80% power and $\alpha = 0.05$, 6–8 animals/group are required for TTC staining.

4.3. Mouse model of focal cerebral ischemia and reperfusion

Focal cerebral ischemia was induced by transient middle cerebral artery occlusion (tMCAO) using an intraluminal monofilament technique as described previously.(Begum et al., 2015; Dharap et al., 2009) Briefly, randomized WT or KI mice (18–20 g) were kept anesthetized under 1% isoflurane at 37 °C. After isolating the right common carotid artery (CCA), the right external carotid artery (ECA), and the right internal carotid artery (ICA), a 7–0 suture was tied at the origin and at the distal end of the ECA. A 6–0 fine MCAO suture (602156PK10, filament size 6–0, diameter 0.09–0.11 mm, length 20 mm; diameter with coating 0.21 +/− 0.02 mm, Doccol, Sharon, MA) was pushed up the ICA to occlude the origin of the middle cerebral artery (MCA). The suture was removed after 1 h to allow reperfusion for 24 h. After reperfusion, the mice were sacrificed and the brains were removed and serial coronal brain sections (1 mm apart) were obtained and stained with 2, 3, 5-triphenyltetrazolium chloride monohydrate (TTC; Sigma-Aldrich, St. Louis, MO, USA) for assessing size of infarction. The regions of brain section stained red are the live tissues, while the unstained white regions are indicative of dead tissue/infarction. Infarction volume was quantified using ImageJ 1.53. Quantification was performed on each brain slice to determine the cortical, striatal, and total infarction volume of each mouse. For cryostat sectioning, mice were perfused with 4% paraformaldehyde before isolating the brain. Tissues from the ischemic core and surrounding the PI regions, striatum, hippocampus were dissected and snap-frozen in dry ice for Western blotting and QPCR analysis.

A 39-point neurological score test was also performed blindly on each mouse at 24 h after MCAO (De Simoni et al., 2003). The test evaluates each mouse's neurological and motor functioning using 13 criteria including hair (score 0–2), eyes (score 0–3), spontaneous activity (score 0–3), body symmetry (score 0–2), circling behavior (score 0–3), gait (0–4), Ears (score 0–2), whisker response (score 0–4), forelimb symmetry (score 0–4), compulsory circling (score 0–3), posture (score 0–3), climbing (score 0–3), gripping test of the forepaws (score 0–3). The scoring range is 0 (lowest) to 39 (highest).

4.4. Quantitative real time PCR

Total RNA was isolated from primary cortical neuronal cultures, brain tissues, or N2a cells, by using Trizol (Invitrogen, Carlsbad, CA). Quantitative real-time reverse-transcriptase polymerase chain reaction (RT-PCR) was carried out with a Bio-Rad CFX Connect thermocycler, iScript cDNA synthesis kit, and iTaq Universal SYBR green supermix (Bio-Rad, Hercules, CA). The relative mRNA expression was normalized to Cyclophilin mRNA

levels. PCR experiments were repeated 3 times, each using separate sets of cultures. The qPCR primer sequences are: 1 mouse *Prkd1*: 5′-CGGATCCAACTCACACAAAGAT-3′ (sense), 5′-AACTGTCCGGAACCCAGAAC-3′ (antisense); mouse *Prkd2*: 5′-GTCCGTGGGTGTGATCATGT-3′ (sense), 5′-GGTCGATGGCTCCAGATGAG-3′ (antisense); mouse *Prkd3*: 5′-TGAGGTTCCCCACAAAGCAA-3′ (sense), 5′-CGAAGACTCGTTCTGGGGTT-3′ (antisense); mouse Cyclophilin: 5′-ACTCCTCATTTAGATGGGCATCA-3′ (sense), 5′-GAGTATCCGTACCTCCGCAAA-3′ (antisense);

4.5. Cell cultures and oxygen-glucose deprivation (OGD)

Mouse N2A (N2A) cells were purchased from American Type Culture Collection (CCL-131, ATCC, Manassas, VA). ATCC performed authentication for these cell lines using short tandem repeat profiling. N2A cells were grown to 85–95% confluency before using for studies. To prepare primary cortical neurons, dissection of the cortex was performed on embryonic 18-day old rats and mice. Briefly, papain solution (Worthington, Lakewood, NJ) and subsequent trypsin inhibitor solution (Worthington) were applied and removed from the cells before neurons were plated and maintained in Neurobasal medium (Invitrogen, Carlsbad, CA). After plating in poly-D-lysine (Sigma-Aldrich, St. Louis, MO) coated dishes, neurons were cultured *in vitro* 14 days before OGD/R treatment.

To model ischemia-like conditions *in vitro*, N2a and primary cortical neurons were subjected to *in vitro* ischemia by oxygen and glucose deprivation for 3 h (N2a) or 1 h (primary neurons) by use of hypoxia chamber and glucose-free medium, followed by incubation in glucose-containing medium under normoxic conditions in 37 °C incubator for various times (Lenart et al., 2004). In some experiments, N2A cultures were treated with DMSO or CRT0066101 at 2 or 5 μM for 45 min prior to and during OGD exposure and subsequently during reoxygenation.

4.6. OGD/R-induced cell viability assays

For primary neurons, cell viability was determined before, right after, or 24 h after OGD treatment using calcein-AM and propidium iodide (PI) staining. In accordance with the manufacturer's protocol, cells were washed with PBS once before being subjected to 200 nM calcein-AM (65085339; Invitrogen) and 1 μg/ml PI (P3566; Molecular Probes) staining for 30 min at 37 °C for 30 min. Culture dishes were examined under an Olympus 1 × 71 inverted system microscope with 10× objective lens. Three to four images were taken randomly from each culture dish. For quantification, three individual experiments were performed with live and dead cells counted using ImageJ v1.53.

To measure viability of N2a cells, the cells were infected with NucLight Red Lentivirus reagent (Satorius, Bohemia, NY) to establish a stable N2a-NR cell line expressing red fluorescent protein mKate2. N2a-NR cells were seeded at 80,000 cells/well in 24-well plates in growth medium containing 10% FBS. After inhibitor and OGD treatment, the plates were placed in the IncuCyte S3 Live Cell Imaging System (Satorius) where real-time images were captured every 6 h for 4–7 days at 10X magnification throughout the experiment. The red fluorescent signal of cells was analyzed using IncuCyte cell-by-cell module (Satorius).

4.7. Immunofluorescent staining and image analysis

At 24 h following MCAO, PKD2-KI and WT mice were anesthetized with 1% isoflurane and transcardially perfused with 1× PBS followed by 4% paraformaldehyde in PBS. Brains were harvested and cryoprotected in 30% sucrose in PBS, and frozen serial coronal brain sections (35 μm thick) were prepared on a cryostat (CM1850 UV, LEICA). Brain sections were blocked with 5% normal goat serum in PBS for 1 h, followed by overnight incubation (4 °C) with the following primary antibodies: rabbit anti-NeuN (1:500; EMD Millipore), anti-PKD2 (1:200), anti-p-S876-PKD2 (1:200), and counterstained with DAPI. Secondary antibodies: Cy3-conjugated goat anti-rat IgG, Alexa Fluor 488-conjugated goat anti-rabbit IgG and goat anti-mouse IgG (all at 1:500; The Jackson ImmunoResearch Lab). Images were collected by confocal microscopy (FV1000-II; Olympus) and processed in Adobe Photoshop for compositions.

4.8. Plasmid transfection

The pcDNA-DYK-mPKD2 plasmid was obtained from GeneScript (Piscataway, NJ). N2a cells were transfected using TurboFect transfection reagent according to the manufacturer's instructions (Thermo Fisher). Cells were used for experiments 24–48 h after transfection.

4.9. Western blot analysis

Cells or tissues were lysed in lysis buffer (50 mM Tris-HCl, pH 7.4, 150 mM NaCl, 1.5 mM $MgCl_2$, 10% Glycerol, 1% Triton X-100, 5 mM EGTA, 20 uM leupeptin, 1 mM AEBSF, 1 mM $NaVO_3$, 10 mM NaF, and 1× protein inhibitor cocktail). Western blot analysis was carried out as previously reported.(Chen et al., 2008) Briefly, cell lysates were run on SDS-PAGE gels and transferred onto PVDF membranes. After pre-blocking, the membranes were incubated with the appropriate primary antibodies at 4 °C overnight. After washing, the membranes were incubated with secondary antibodies at room temperature for 1 h. Protein bands were detected with the enhanced chemiluminescence (ECL) kit. The images were captured on X-ray film and the band intensity was quantified by ImageJ 1.53 software.

4.10. Statistical analysis

Statistical analysis was performed using GraphPad Prism 9 software (GraphPad Software, La Jolla, CA). The data were examined for normal or lognormal distributions. If the criteria for normal distribution were not met, non-parametric test was performed. Analysis of differences between two groups with similar variances was performed using Student's *t*-test (two-tailed). The experimental groups compared statistically in this study showed similar variances. In case of three or more groups, one-way ANOVA followed by multiple-comparison tests was used. The sample sizes in our experiments were shown in the legends. They were based on previous experimental observations, not pre-determined by statistical methods. No samples were excluded from the analysis in this work. For the animal study, mice died during or after MCAO surgery were excluded from the experimental groups. Blinding method was utilized to avoid bias. Values are presented as the mean ± standard error of the mean (SEM) of at least three independent experiments. Replicate experiments will be analyzed both independently and jointly, controlling for batch effects. A p value

<0.05 was considered statistically significant (*, $P < 0.05$; **, $P < 0.01$; ***, $P < 0.001$; ****, $P < 0.0001$; ns, not significant).

Funding statement

This work was supported in part by the American Heart Association award 19TPA34850096 (Wang) and R01MH114908 (Jacob).

Acknowledgements

We are truly thankful for Daniela Guerrero from the Summer Undergraduate Research Program at Department of Pharmacology and Chemical Biology, University of Pittsburgh, for her technical assistance in the completion of an overexpression experiment. We are grateful to Caitlyn Chapman, Jessica Nuwer, and Jacob Lombardi from the laboratory of Tija C. Jacob for their training of the cortical neuron dissection process and supply of rat cortical neurons.

Data availability

All data generated or analyzed during this study are included in this published article and its supplementary information files.

Abbreviations:

PKD	protein kinase D
tMCAO	transient middle cerebral artery occlusion
WT	wild-type
I/R	ischemia/reperfusion
tPA	tissue plasminogen activator
DAG	diacylglycerol
PKC	protein kinase C
HSP90	heat shock protein 90
IF	immunofluorescent
CCA	common carotid artery
ECA	external carotid artery
ICA	internal carotid artery
MCA	middle cerebral artery
RT-PCR	reverse-transcriptase polymerase chain reaction
PI	propidium iodide
ECL	enhanced chemiluminescence

PKD2-KI	kinase-dead PKD2 knock-in
OGD/R	oxygen-glucose deprivation/reoxygenation
TTC	2,3,5-triphenyltetrazolium chloride monohydrate
CRT	CRT0066101
HSP27	heat-shock protein 27
NMDARs	*N*-methyl-D-aspartate receptors

References

Atik N, et al. , 2014. The role of PKD in cell polarity, biosynthetic pathways, and organelle/F-actin distribution. Cell Struct. Funct 39, 61–77. [PubMed: 24492625]

Avriyanti E, et al. , 2015. Functional redundancy of protein kinase D1 and protein kinase D2 in neuronal polarity. Neurosci. Res 95, 12–20. [PubMed: 25639845]

Azoitei N, et al. , 2014. HSP90 supports tumor growth and angiogenesis through PRKD2 protein stabilization. Cancer Res. 74, 7125–7136. [PubMed: 25297628]

Begum G, et al. , 2015. Inhibition of WNK3 kinase signaling reduces brain damage and accelerates neurological recovery after stroke. Stroke. 46, 1956–1965. [PubMed: 26069258]

Bright R, Mochly-Rosen D, 2005. The role of protein kinase C in cerebral ischemic and reperfusion injury. Stroke. 36, 2781–2790. [PubMed: 16254221]

Burciaga SD, et al. , 2023. Protein kinase D3 conditional knockout impairs osteoclast formation and increases trabecular bone volume in male mice. Bone. 172, 116759. [PubMed: 37044359]

Chandra PK, et al. , 2021. Transcriptome analysis reveals sexual disparities in gene expression in rat brain microvessels. J. Cereb. Blood Flow Metab. 41, 2311–2328. [PubMed: 33715494]

Chen J, et al. , 2008. Protein kinase D3 (PKD3) contributes to prostate cancer cell growth and survival through a PKCepsilon/PKD3 pathway downstream of Akt and ERK 1/2. Cancer Res. 68, 3844–3853. [PubMed: 18483269]

Chen L, et al. , 2023. Loss of protein kinase D2 activity protects against bleomycin-induced dermal fibrosis in mice. Lab. Invest 103, 100018. [PubMed: 37039152]

De Simoni MG, et al. , 2003. Neuroprotection by complement (C1) inhibitor in mouse transient brain ischemia. J. Cereb. Blood Flow Metab 23, 232–239. [PubMed: 12571454]

Dharap A, et al. , 2009. Transient focal ischemia induces extensive temporal changes in rat cerebral microRNAome. J. Cereb. Blood Flow Metab 29, 675–687. [PubMed: 19142192]

Gallizioli M, et al. , 2023. Differences in the post-stroke innate immune response between young and old. Semin. Immunopathol 45, 367–376. [PubMed: 37045990]

Ge Y, et al. , 2020. NMDARs in cell survival and death: implications in stroke pathogenesis and treatment. Trends Mol. Med 26, 533–551. [PubMed: 32470382]

Guo J, et al. , 2011. Protein kinase D isoforms are activated in an agonist-specific manner in cardiomyocytes. J. Biol. Chem 286, 6500–6509. [PubMed: 21156805]

Harikumar KB, et al. , 2010. A novel small-molecule inhibitor of protein kinase D blocks pancreatic cancer growth in vitro and in vivo. Mol. Cancer Ther 9, 1136–1146. [PubMed: 20442301]

Higuero AM, et al. , 2010. Kidins220/ARMS modulates the activity of microtubule-regulating proteins and controls neuronal polarity and development. J. Biol. Chem 285, 1343–1357. [PubMed: 19903810]

Jia C, et al. , 2022. Female-specific neuroprotection after ischemic stroke by vitronectin-focal adhesion kinase inhibition. J. Cereb. Blood Flow Metab 42, 1961–1974. [PubMed: 35702047]

Johannessen M, et al. , 2007. Protein kinase D induces transcription through direct phosphorylation of the cAMP-response element-binding protein. J. Biol. Chem 282, 14777–14787. [PubMed: 17389598]

Kitagawa K, 2007. CREB and cAMP response element-mediated gene expression in the ischemic brain. FEBS J. 274, 3210–3217. [PubMed: 17565598]

Lenart B, et al. , 2004. Na-K-Cl cotransporter-mediated intracellular Na+ accumulation affects Ca2+ signaling in astrocytes in an in vitro ischemic model. J. Neurosci 24, 9585–9597. [PubMed: 15509746]

Li G, Wang Y, 2014. Protein kinase D: a new player among the signaling proteins that regulate functions in the nervous system. Neurosci. Bull 30, 497–504. [PubMed: 24526660]

Liu J, et al. , 2022. Sexual dimorphism in immune cell responses following stroke. Neurobiol. Dis 172, 105836. [PubMed: 35932990]

Maier D, et al. , 2019. Protein kinase D is dispensable for development and survival of *Drosophila melanogaster*. G3 (Bethesda) 9, 2477–2487. [PubMed: 31142547]

Matsumura K, et al. , 2019. Autism-associated protein kinase D2 regulates embryonic cortical neuron development. Biochem. Biophys. Res. Commun 519, 626–632. [PubMed: 31540692]

Matthews SA, et al. , 2010. Unique functions for protein kinase D1 and protein kinase D2 in mammalian cells. Biochem. J 432, 153–163. [PubMed: 20819079]

Oster H, et al. , 2006. Expression of the protein kinase D (PKD) family during mouse embryogenesis. Gene Expr. Patterns 6, 400–408. [PubMed: 16377259]

Pose-Utrilla J, et al. , 2017. Excitotoxic inactivation of constitutive oxidative stress detoxification pathway in neurons can be rescued by PKD1. Nat. Commun 8, 2275. [PubMed: 29273751]

Sakamuri SS, et al. , 2022. Aging related impairment of brain microvascular bioenergetics involves oxidative phosphorylation and glycolytic pathways. J. Cereb. Blood Flow Metab 42, 1410–1424. [PubMed: 35296173]

Sanchez-Ruiloba L, et al. , 2014. Protein kinase D interacts with neuronal nitric oxide synthase and phosphorylates the activatory residue serine 1412. PLoS One 9, e95191. [PubMed: 24740233]

Sommer CJ, Schabitz WR, 2021. Principles and requirements for stroke recovery science. J. Cereb. Blood Flow Metab 41, 471–485. [PubMed: 33175596]

Stetler RA, et al. , 2008. Hsp27 protects against ischemic brain injury via attenuation of a novel stress-response cascade upstream of mitochondrial cell death signaling. J. Neurosci 28, 13038–13055. [PubMed: 19052195]

Stetler RA, et al. , 2012. Phosphorylation of HSP27 by protein kinase D is essential for mediating neuroprotection against ischemic neuronal injury. J. Neurosci 32, 2667–2682. [PubMed: 22357851]

Storz P, Toker A, 2003. Protein kinase D mediates a stress-induced NF-kappaB activation and survival pathway. EMBO J. 22, 109–120. [PubMed: 12505989]

Sturany S, et al. , 2002. Mechanism of activation of protein kinase D2(PKD2) by the CCK (B)/gastrin receptor. J. Biol. Chem 277, 29431–29436. [PubMed: 12058027]

Tang BL, 2001. Protein trafficking mechanisms associated with neurite outgrowth and polarized sorting in neurons. J. Neurochem 79, 923–930. [PubMed: 11739603]

Wang QJ, Wipf P, 2023. Small molecule inhibitors of protein kinase D: early development, current approaches, and future directions. J. Med. Chem 66, 122–139. [PubMed: 36538005]

Wang R, et al. , 2021. Impact of sex and APOE epsilon4 on age-related cerebral perfusion trajectories in cognitively asymptomatic middle-aged and older adults: a longitudinal study. J. Cereb. Blood Flow Metab 41, 3016–3027. [PubMed: 34102919]

Watkins JL, et al. , 2008. Phosphorylation of the Par-1 polarity kinase by protein kinase D regulates 14–3-3 binding and membrane association. Proc. Natl. Acad. Sci. U. S. A 105, 18378–18383. [PubMed: 19011111]

Wei N, et al. , 2014. Protein kinase d as a potential chemotherapeutic target for colorectal cancer. Mol. Cancer Ther 13, 1130–1141. [PubMed: 24634417]

Wu QJ, Tymianski M, 2018. Targeting NMDA receptors in stroke: new hope in neuroprotection. Mol. Brain 11, 15. [PubMed: 29534733]

Yang SH, Liu R, 2021. Four decades of ischemic penumbra and its implication for ischemic stroke. Transl. Stroke Res 12, 937–945. [PubMed: 34224106]

Yin DM, et al. , 2008. Both the establishment and maintenance of neuronal polarity require the activity of protein kinase D in the Golgi apparatus. J. Neurosci 28, 8832–8843. [PubMed: 18753385]

Yousufuddin M, Young N, 2019. Aging and ischemic stroke. Aging (Albany NY) 11, 2542–2544. [PubMed: 31043575]

Zhang L, et al. , 2017. Androgen suppresses protein kinase D1 expression through fibroblast growth factor receptor substrate 2 in prostate cancer cells. Oncotarget. 8, 12800–12811. [PubMed: 28077787]

Zhang X, et al. , 2021. Multifaceted functions of protein kinase D in pathological processes and human diseases. Biomolecules. 11.

Zhao Y, et al. , 2022. Neuronal injuries in cerebral infarction and ischemic stroke: from mechanisms to treatment (review). Int. J. Mol. Med 49.

Zhou X, et al. , 2014. Protein kinase D2 promotes the proliferation of glioma cells by regulating Golgi phosphoprotein 3. Cancer Lett. 355, 121–129. [PubMed: 25218347]

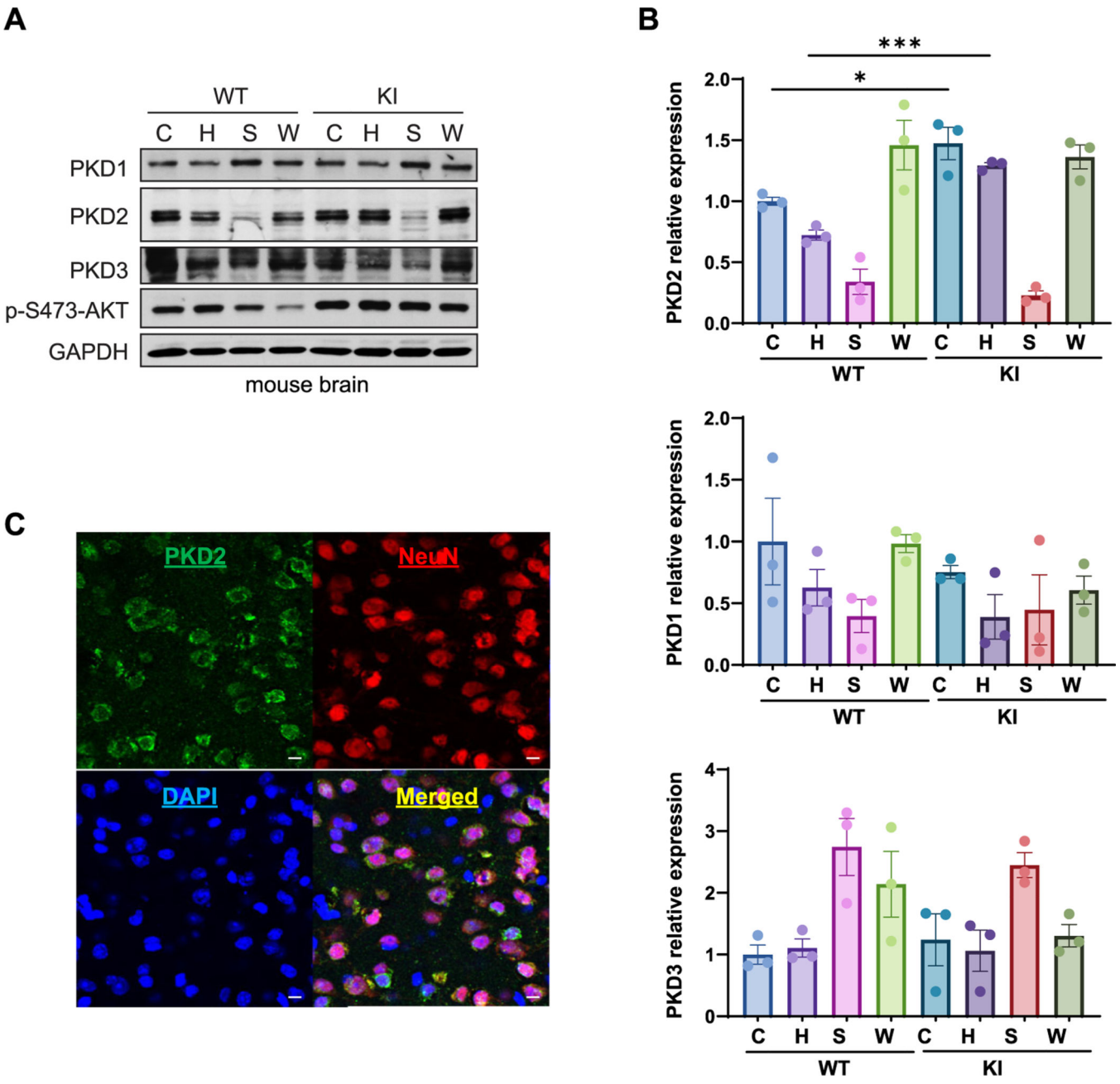

Fig. 1.

The expression of PKD1–3 in WT and KI mouse brain tissues. A-B. PKD1–3 proteins can be detected in mouse brain. WT and KI mouse brain cortex, striatum, and hippocampus tissues were isolated. The tissue extracts were subjected to Western blot analysis for PKD1–3. GAPDH was blotted as the loading control. Representative images from at least three experiments are shown. Quantification on PKD1–3 expression by densitometry analysis (B). C. IF staining of PKD2 and NeuN in mouse cortex ($n = 3$). Nuclei was counterstained by DAPI. Scale bar = 20 μM. Representative images are shown. C, cortex; H, hippocampus; S, striatum; W, whole brain. *$P < 0.05$; ***$P < 0.001$; ns, not significant.

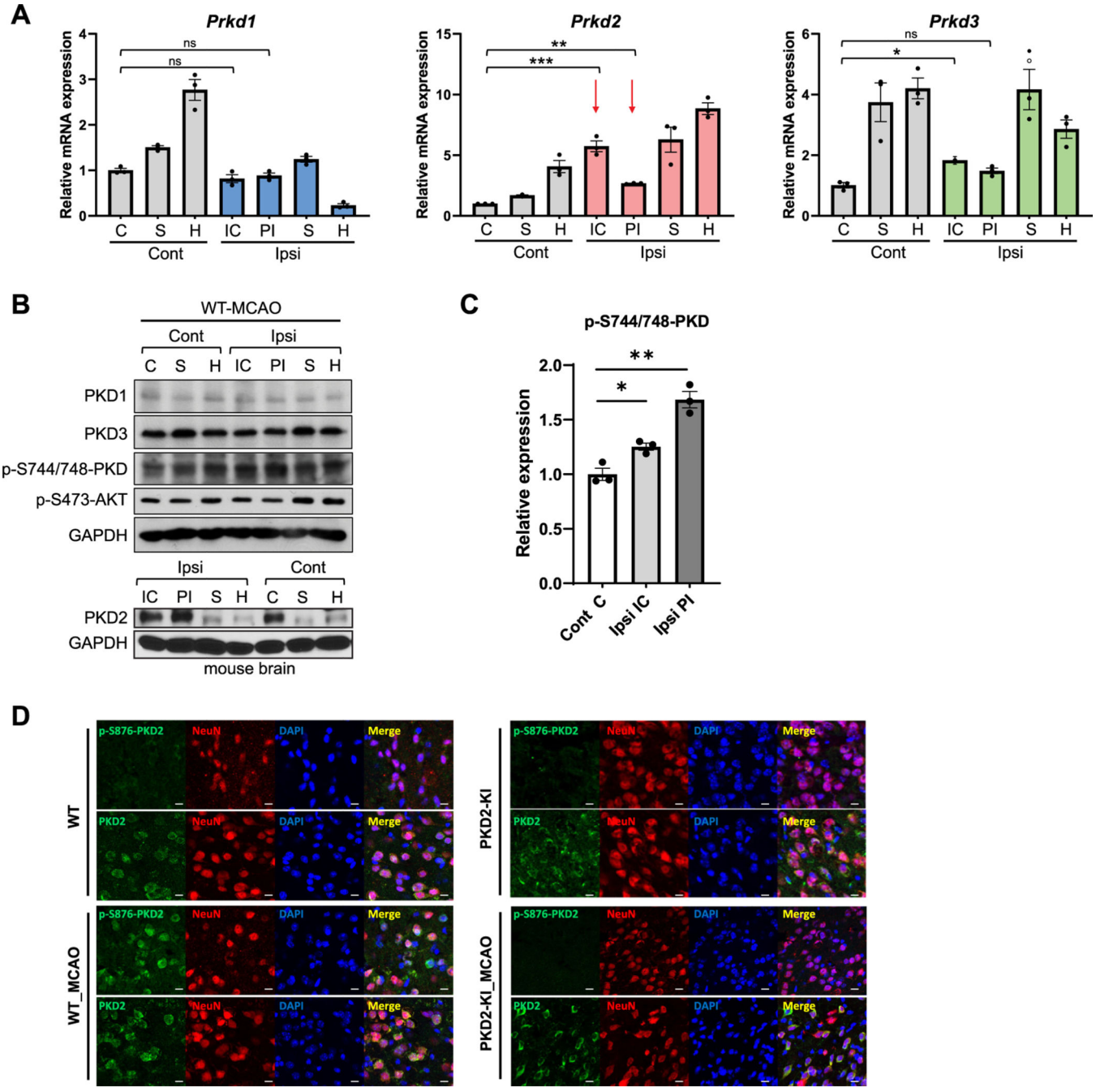

Fig. 2.

Focal ischemia induces upregulation of PKD2 protein and activity in the peri-infarct regions after tMCAO. A. PKD2 was upregulated in ipsilateral tissues. QPCR analysis was used to identify *Prkd1–3* mRNA expression in contralateral and ipsilateral sides of mouse brain at 24 h reperfusion after 1 h MCAO. Data are Mean ± SEM of triplicate determinations from a representative experiment of three such similar experiments. C, cortex; H, hippocampus; S, striatum; IC, ischemic core, PI, peri-infarct; Cont, contralateral; Ipsi, Ipsilateral. B. WT mouse brain tissue subjected to 24 h reperfusion after 1 h MCAO was dissected

and subjected to Western blot analysis followed by immunoblotting for several targets. Representative images from three experiments are shown. C. The activity of PKD increased in the ipsilateral ischemic tissue (cortex and PI) compared to the control tissue in the contralateral cortex. Quantification of p-S744/748-PKD in the Western blots shown in “B” and performed by densitometry analysis. GAPDH was blotted as the loading control. D. The endogenous expression and activity of PKD2 in the peri-infarct area of WT and KI subjected to 1 h MCAO followed by 24 h reperfusion. Mouse brain sections from WT and KI mice were stained for PKD2 and p-S876-PKD2 by IF. Scale bar = 20 μM. Representative images from three experiments are shown. *$P < 0.05$; **$P < 0.01$; ***P < 0.001; ns, not significant.

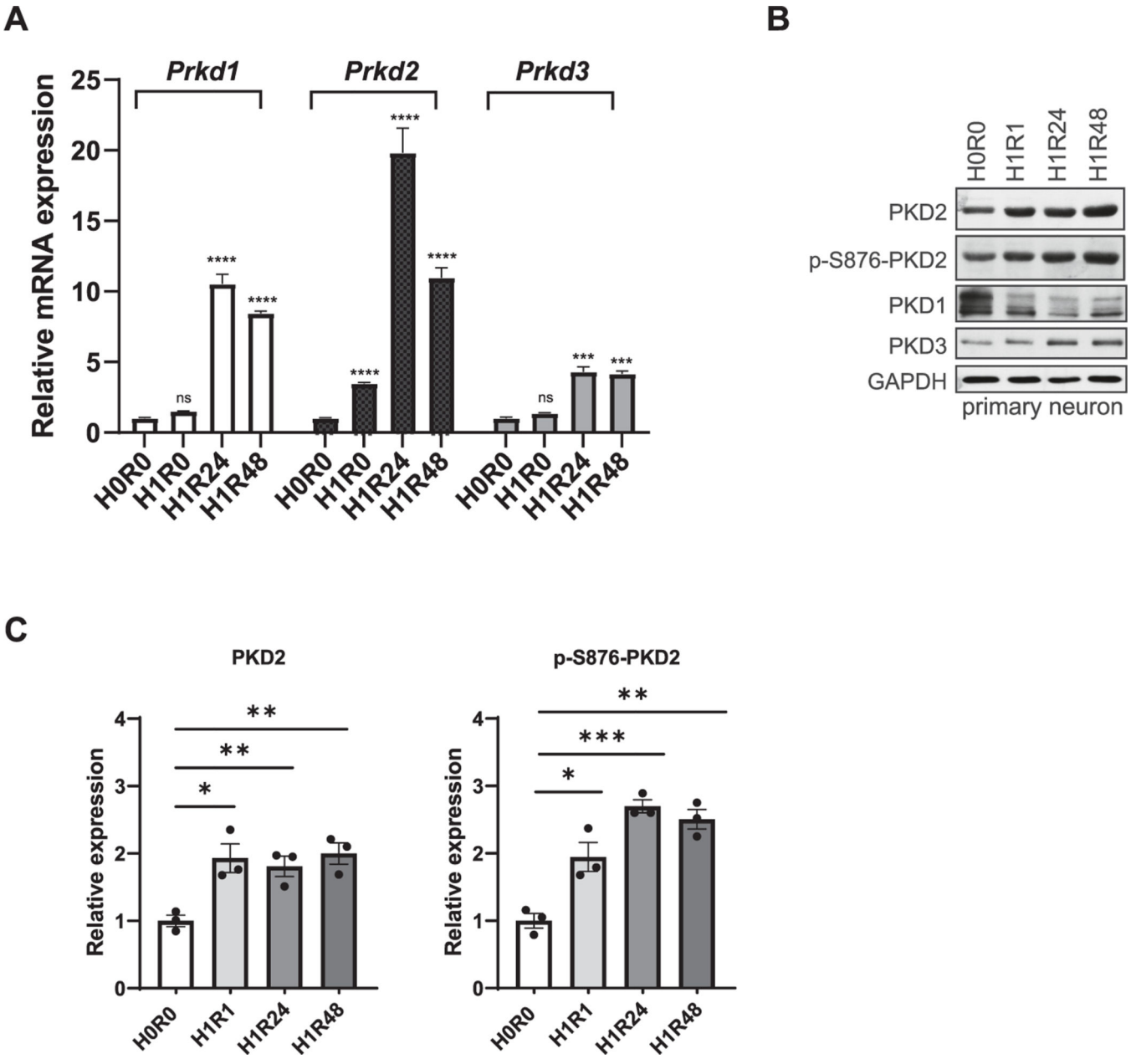

Fig. 3.

Upregulation of PKD2 protein and activity in the primary cortical neuron cultures after OGR/R. A. OGD/R induced the upregulation of PKD2 mRNA. QPCR analysis was used to identify *Prkd1–3* mRNA expression before and after OGD/R in rat primary cortical neurons. B-C. PKD2 expression and activity were both increased in response to OGD/R. PKD1–3 and p-PKD2 expression were analyzed by Western blotting before and after OGD/R in rat primary cortical neurons. GAPDH was blotted as the loading control. Quantification on PKD2 expression and activity was performed by densitometry analysis (C). Representative images from three or more experiments are shown. *$P < 0.05$; **$P < 0.01$; ***$P < 0.001$; ****$P < 0.0001$; ns, not significant.

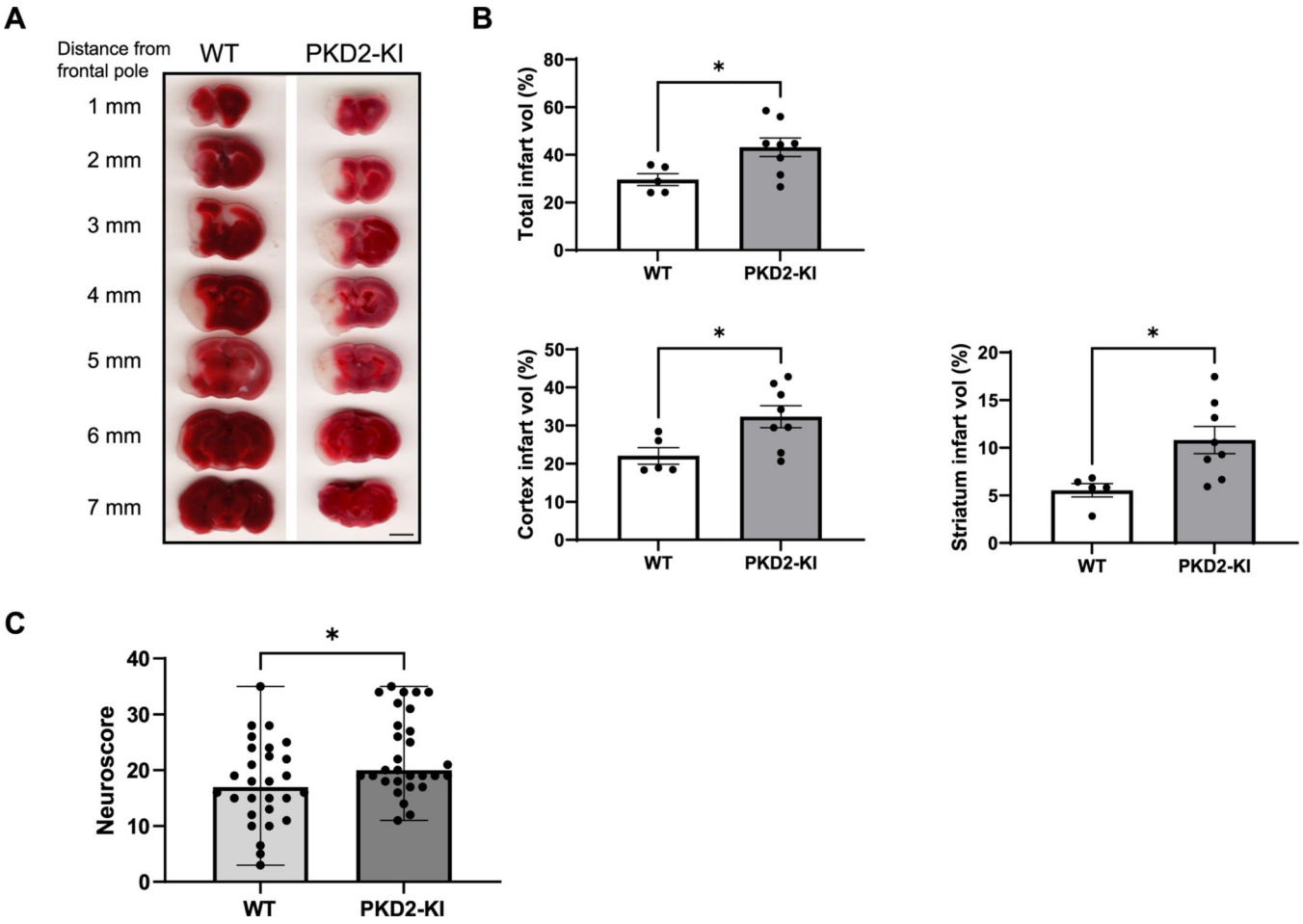

Fig. 4.

PKD2-KI mice exhibit enlarged brain infarction and worse neurological scores after tMCAO. A. PKD2-KI ($n = 8$) and WT mice ($n = 5$) were subjected to 1-h MCAO followed by 24-h reperfusion. TTC-stained coronal sections (1 mm) are shown at different brain levels posterior to the frontal pole. Scale bar = 3 mm. B. Increased infarction volumes were observed in PKD2-KI as compared to WT. Infarct volumes (total, cortex, and striatum) were quantified using ImageJ on TTC-stained WT and PKD2-KI coronal sections. Data are presented as Mean ± SEM from 5 to 8 mice in each group. *$P < 0.05$. C. PKD2-KI mice exhibited worsened neurological scores. Neurological motor functioning was assessed at 24 h reperfusion after MCAO. A nonparametric Mann-Whitney test was performed (*P < 0.05). Data are presented as median/range.

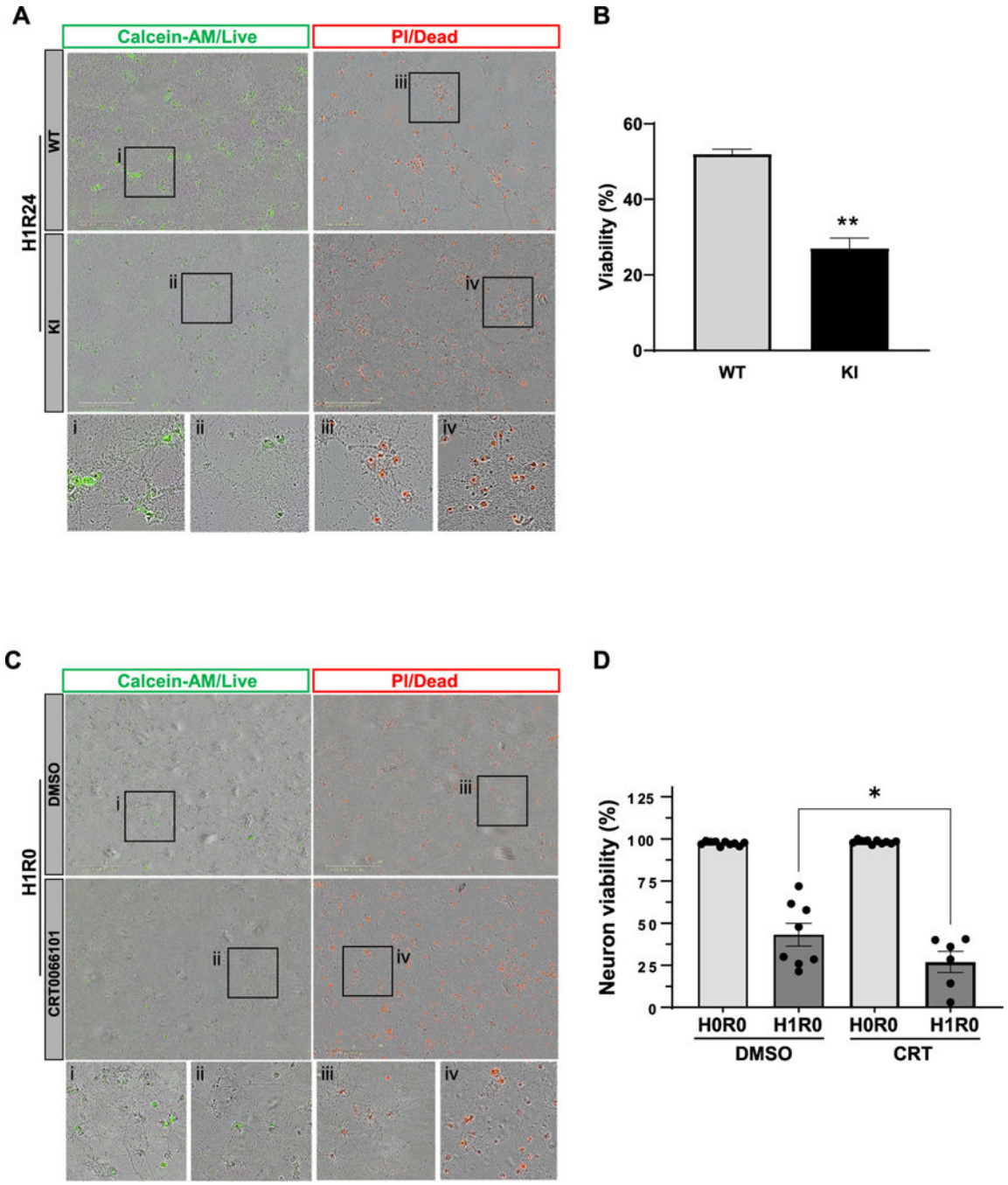

Fig. 5.

Loss of PKD2 or inhibition of PKD increases neuronal death in response to OGD/R in murine primary neurons. A. The KI neurons were less viable than the WT neurons. Survival of WT and PKD2-KI mouse primary cortical neurons after OGD/R treatment at H1R24 (*n* = 4). Neuron viability was measured by Calcein-AM/PI staining. Composite phase/Calcein AM or phase/PI images are shown. B. Quantification of cell viability at H1R24 in "A". C. PKD inhibition increased neuronal death compared to vehicle treatment during OGD/R. Survival of rat primary cortical neurons at H1R0 treated with or without CRT (2 μM). CRT

was added throughout OGD/R treatment. D. Quantification of cell viability in “C”. For all, representative images are shown. i-iv are enlarged sections within the square box. Scale bar, 400 μm. Magnification, 10×. Data are Mean ± SEM from at least three experiments. **P < 0.01; ***$P < 0.001$.

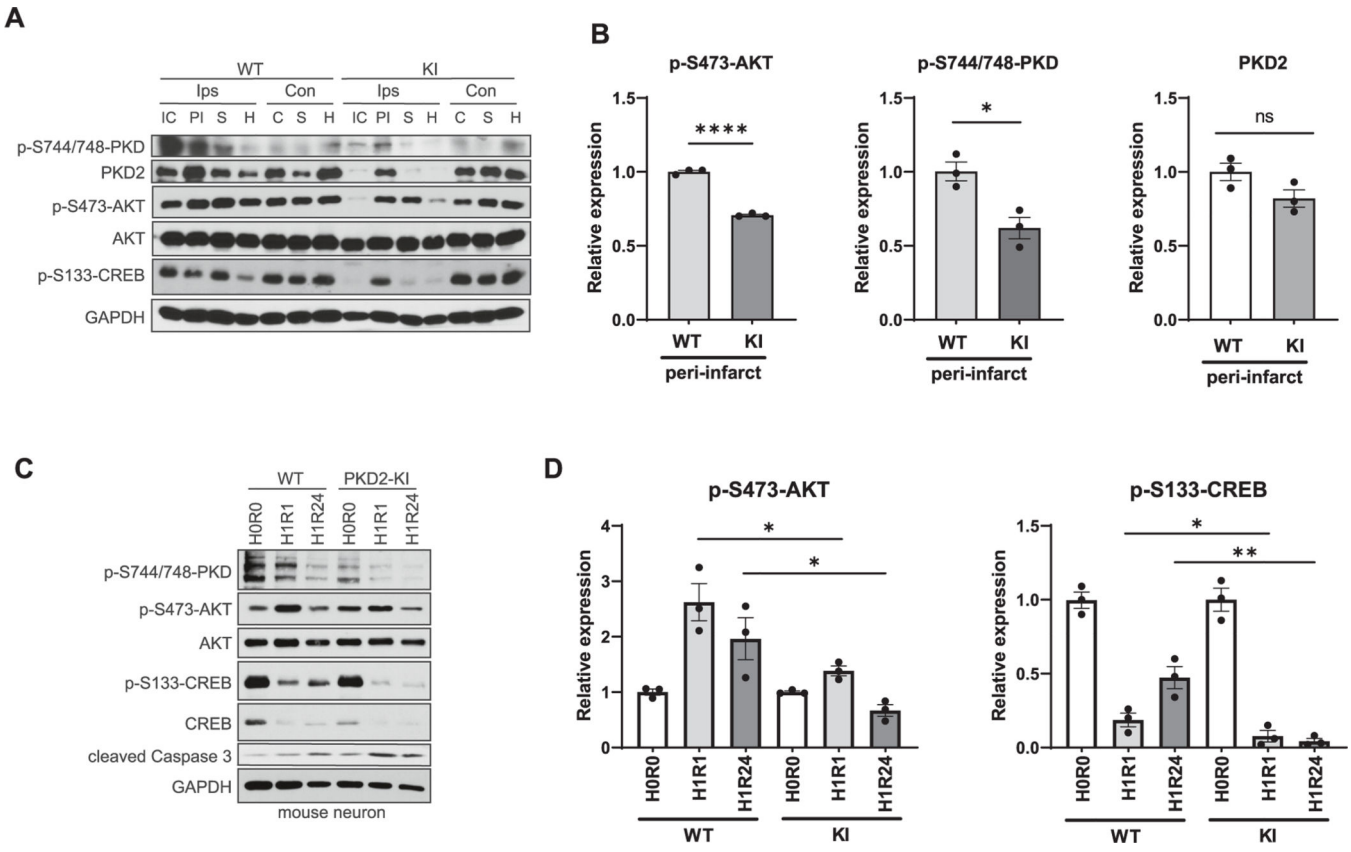

Fig. 6.

Inactivation of PKD2 attenuates AKT and CREB activities during I/R. A. PKD and AKT activity decreased in PKD2-KI ipsilateral peri-infarct tissues. Western blot analysis of dissected mouse brain tissue (WT and PKD2-KI) after 1 h transient ischemia and 24 h reperfusion. GAPDH was blotted as the loading control. C, cortex; H, hippocampus; S, striatum; IC, ischemic core, PI, peri-infarct; Cont, contralateral; Ipsi, Ipsilateral. B. Quantification on selected targets in the Western blots shown in “A” by densitometry analysis. C. AKT and CREB activities decreased in PKD2-KI cortical neurons compared to the WT. Western blotting analysis of primary mouse neuron from WT and PKD2-KI mice subjected to OGD/R treatment. D. Quantification of p-S473-AKT and p-S133-CREB levels in the Western blots shown in “C” by densitometry analysis. Representative images from three or more experiments are shown. *P < 0.05; **P < 0.01; ****P < 0.0001; ns, not significant.

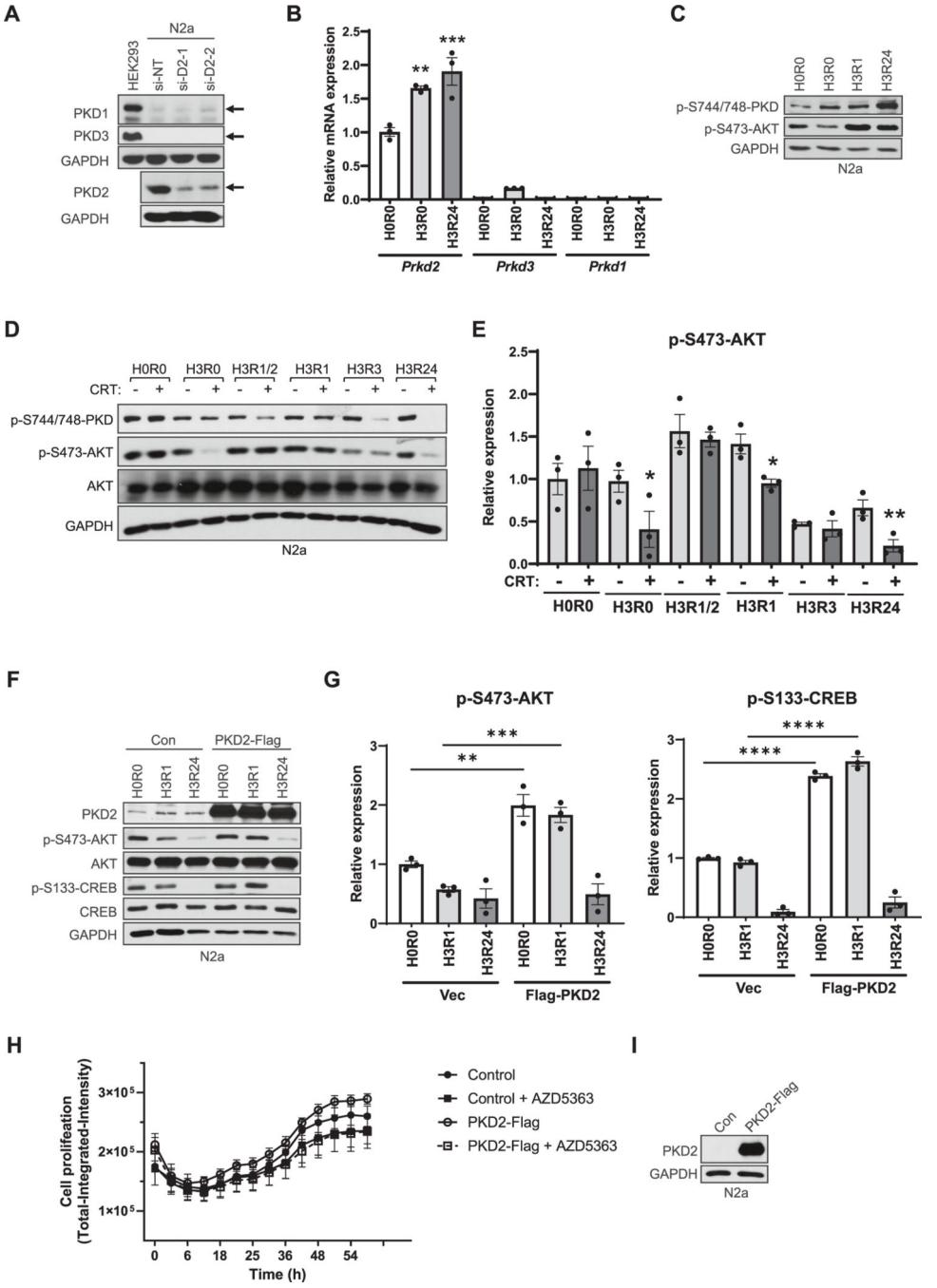

Fig. 7.

PKD2 regulates AKT and CREB activities in N2a cells after OGD/R. A. PKD2 was the only PKD isoform expressed in N2a. N2a cells were transfected with a non-targeting (si-NT) and two different PKD2 siRNAs (si-D2–1 and si-D2–2). Cell lysates were analyzed by Western blot analysis, followed by immunoblotting for PKD1–3. HEK293 was used as a control. B. OGD/R upregulated PKD2 but not PKD1 and 3 mRNAs in N2a cells. Cell lysates were subjected to OGD/R, followed by QPCR analysis for PKD1–3 mRNAs. C. OGD/R upregulated PKD (primarily PKD2) activity in N2a cells. Western blot analysis of

N2a cells before and after OGD/R treatment. D. Inhibition of PKD blocked OGD/R-induced AKT activation. Western blot analysis of N2a cells subjected to OGD/R for various times without or with CRT (5 μM). E. Quantification of p-S473-AKT in “D” by densitometry analysis. F. PKD2 overexpression increased p-S473-AKT and p-S133-CREB levels after OGD/R in N2a cells. N2a cells were transfected with a Flag-tagged PKD2 (PKD2-Flag) or an empty vector (Con). After 24 h, the cells were subjected to OGD/R treatment, followed by immunoblotting for the indicated targets. G. Quantification on p-S473-AKT and p-S133-CREB shown in “F” by densitometry analysis. H. Time-course of N2a-NR cells expressing vector control or PKD2-Flag and treated with or without an AKT inhibitor AZD5363 (1 μM). Total integrated intensity was measured by IncuCyte live-cell imaging. Data from one of three representative experiments are shown. I. Westen blotting confirmed the overexpression of PKD2-Flag in N2a-NR cells used in “H”. For all, representative Western blot images and data from at least three experiments are shown. GAPDH was blotted as the loading controls. *P < 0.05; **P < 0.01; ***P < 0.001; ****P < 0.0001; ns, not significant.